Direct imaging of multimode interference in a channel waveguide

A. L. Campillo*

Bell Laboratories, Lucent Technologies, Murray Hill, New Jersey 07974, and University of Virginia, Charlottesville, Virginia 22904

J. W. P. Hsu

Bell Laboratories, Lucent Technologies, Murray Hill, New Jersey 07974

K. R. Parameswaran and M. M. Fejer

Stanford University, Stanford, California 94305

Received August 6, 2002

By use of a near-field scanning optical microscope in collection mode, multimode interference was directly measured in an annealed proton-exchanged $LiNbO_3$ waveguide. Periodic transitions from a single-peaked Gaussianlike intensity distribution to a double-peaked intensity distribution were observed. The intensity distribution along the waveguide was calculated, and the results agree well with the experimental observation. © 2003 Optical Society of America

OCIS codes: 180.5810, 130.3120, 130.3730, 130.2790, 260.3160, 230.7380.

Couplers based on multimode interference imaging, in which interference of modes propagating in a multimode region periodically produce single and multiple images of the input mode, are increasingly used to couple and divide light in integrated photonic circuits. These couplers have small device dimensions and high fabrication tolerances compared with those of directional couplers. Beam propagation methods or mode propagation analysis[1] can be used to calculate the locations at which images in a two-dimensional multimode waveguide occur. Indirect experimental observation of multimode imaging in a symmetric waveguiding region was previously done on an erbium-doped Al_2O_3 waveguide by using an optical microscope to image the upconverted green luminescence from Er^+ ions excited by the infrared light propagating through the waveguide.[2] However, this method requires a specially fabricated waveguide and cannot be used to examine real devices. Direct observation of multimode imaging in couplers and waveguides at the operating wavelength(s) will generate data for comparison with design parameters and will greatly enhance the ability to optimize these devices. To our knowledge, such a direct observation of multimode interference has not been reported. One technique that is capable of achieving this goal is collection-mode near-field scanning optical microscopy (NSOM).[3] This technique was previously used to directly map guided light in waveguides,[4–6] ring resonators,[7] and two-dimensional photonic crystals.[8] In this Letter, NSOM is used to directly map multimode interference imaging in an annealed proton-exchanged[9] $LiNbO_3$ waveguide. The experimental results are compared with calculations based on physical parameters of the waveguide and the input mode.

Figure 1 illustrates the experimental setup. The sample studied in this experiment was an ~10-μm-wide waveguide formed by the annealed proton-exchange (APE) process on a z-cut $LiNbO_3$ crystal.[10,11] The width of the waveguide was defined by a channel formed in a SiO_2 mask deposited on the $LiNbO_3$ surface before APE. The sample was proton exchanged to a depth of 0.85 μm, then annealed for 26 h at 328 °C. Light from an infrared diode laser (Santec ECL-200), tunable from 1470 to 1650 nm with a maximum output power of 10–15 mW, was coupled into the waveguide. The sharpened tip of a single-mode optical fiber, fabricated by chemical etching,[12,13] is held ~10 nm above the waveguide surface. The exponentially decaying evanescent tail of the guided light in the waveguide coupled to the fiber tip, and a small portion of the guided light was collected. The collected light was transmitted along the fiber and detected with an InGaAs photodiode (Hamamatsu G3476-03). By holding the tip at a constant height above the sample, using nonoptical shear force feedback[14,15] and raster scanning the tip above the waveguide, we could construct a point-by-point intensity image.

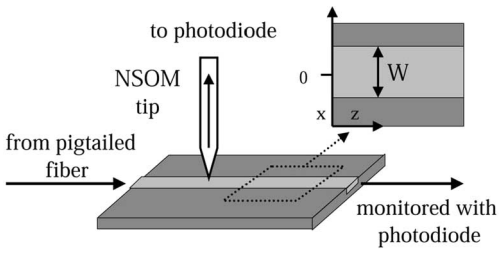

Fig. 1. Experimental setup: Light from an infrared laser is launched into the $LiNbO_3$ waveguide through a single-mode optical fiber pigtail. A small portion of the light is collected by the NSOM tip and detected by a photodiode. Inset, the geometry of the two-dimensional waveguide used in the calculation ($W = 10$ μm).

0146-9592/03/060399-03$15.00/0

NSOM tips are often coated with metal to produce a small (~100-nm), well-defined aperture, improving the spatial resolution. However, since <300-nm resolution was not expected in this experiment, we did not coat the fiber tips with metal to maximize light-collection efficiency. To launch light into the $LiNbO_3$ waveguide, we pigtailed a single-mode optical fiber onto one end of the waveguide, whose facets were polished at an angle of 6° to eliminate standing waves due to backreflection of the light. Since the APE process increases the index of refraction along the extraordinary axis and slightly reduces the index along the ordinary axis, the waveguide supports only TM modes. A fiber polarization controller (not shown in Fig. 1) placed between the laser and the waveguide was used to maximize the waveguide throughput. The power at the waveguide output was monitored with a photodiode. We were unable to measure any change (detection sensitivity $\leq 0.2\%$) in output power as the NSOM tip approached the waveguide surface, indicating that the tip does not strongly perturb the light propagating in the waveguide. The effective index of the fundamental mode of this waveguide was measured by NSOM to be 2.15.[16]

Figure 2 shows two 30 μm × 30 μm NSOM images acquired at nearby positions along the waveguide. We observe an intensity distribution characterized by regular transitions between a Gaussianlike mode with a single peak [left-hand side of Fig. 2(a)] and a symmetric double-peaked distribution [right-hand side of Fig. 2(b)]. The two-peaked distribution and the periodic transitions between the single-peaked and double-peaked structures are the result of multimode interference in the waveguide.[1] This interference arises because the mode from the fiber launches power into multiple modes supported by the $LiNbO_3$ waveguide. The mode of the fiber (measured by taking an NSOM image of its end) has a mean field radius (MFR) of 3.2 μm. This radius does not match that of the fundamental waveguide mode (whose MFR is calculated to be 3.5 μm). Therefore, the light from the fiber excites multiple waveguide modes, which interfere along its length.

To confirm that the experimental observation is due to multimode interference, we performed a calculation of the interference among modes supported in the waveguide. The guided modes of the waveguide were calculated with the semivectorial polarized finite-difference method[17] based on the index profile typical of a waveguide with the same fabrication conditions.[11] The calculation indicates that this waveguide supports three modes: two symmetric and one antisymmetric in width (the x direction). Because the input fiber is centered on the waveguide, we except that the power will be launched primarily into the symmetric modes. The calculated electric fields of the two symmetric modes [$g_1(x)$ and $g_3(x)$] near the surface of the waveguide are shown in Fig. 3(a). The calculated effective indices are $n_1 = 2.145$ and $n_3 = 2.138$. The field [$E(x, z = 0)$] at the entrance of the waveguide is a linear combination of the j symmetric guided modes:

$$
\begin{aligned}
E(x,0) &= \sum_{l=1}^{j} A_l g l(x)\,, \\
A_l &= \frac{1}{N}\int \exp(-x^2/a^2) g_l(x)\mathrm{d}x\,, \\
N_l &= \int \exp(-x^2/a^2)\exp(-x^2/a^2)\mathrm{d}x \int g_l(x) g_l(x)\mathrm{d}x\,,
\end{aligned}
\tag{1}
$$

where a is the MFR of the Gaussian beam entering the waveguide and N_l is a normalization constant. For this calculation, the waveguide was treated as two-dimensional, with the field profiles shown in Fig. 3(a) as the guided modes. The relative intensities of the modes are given by A_l, the normalized projection of the mode in the fiber onto the lth guided mode of the waveguide. As the light propagates along the waveguide, the evolution of the phase of each mode is taken into account by addition of a propagation term:

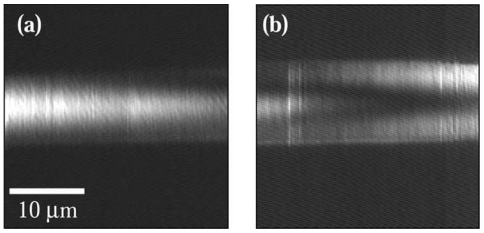

Fig. 2. Two nearby 30 μm × 30 μm intensity images of $\lambda = 1550$ nm light propagating in an APE waveguide patterned on a z-cut $LiNbO_3$ substrate. In (a), a single maxima centered on the waveguide is shown. In (b), a transition from a single peak to symmetric double peaks can be seen.

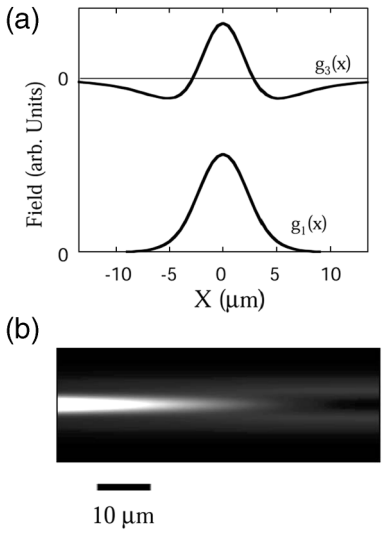

Fig. 3. (a) Surface electric field variation for the two symmetric width modes [$g_1(x)$ and $g_3(x)$] supported by this waveguide, calculated with the semivectoral polarized finite-difference method. The two curves are offset for clarity. (b) 60-μm-long section of the intensity ($|E|^2$) evolution along the waveguide [calculated with Eqs. (1) and (2)] for the two symmetric width modes at $\lambda = 1.55$ μm with $a = 3.2$ μm for the input mode. The transition from a single-peaked Gaussian to a mode with two peaks can be clearly seen.

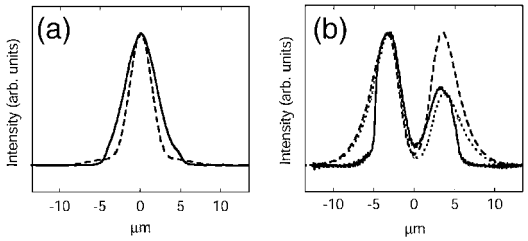

Fig. 4. Cross sections of the NSOM images (solid curves) and calculated distributions (dashed curves), each one normalized to its respective maximum intensity. (a) Single-peaked structure. The solid curve is a cross section of the left-hand edge of Fig. 2(a), and the dashed curve is across the left-hand edge of Fig. 3(b). (b) Double-peaked structure. The solid curve is taken across the right-hand edge of Fig. 2(b), and the dashed curve is taken across the right-hand edge of Fig. 3(b). The dotted curve in (b) shows the calculated distribution for the case in which 5% of the power is launched into the lowest-order antisymmetric guided mode.

$$E(x,z) = \sum_{l=1}^{j} A_l g_l(x) \exp(i\beta_l z)\,, \tag{2}$$

where β_l is the propagation constant of the lth guided mode ($\beta_l = n_l 2\pi/\lambda$).

Figure 3(b) shows a 60-μm-long section of the intensity $|E|^2$ evolution along the waveguide, calculated with Eqs. (1) and (2) for the two symmetric width modes at $\lambda = 1.55$ μm with $a = 3.2$ μm for the input mode. The transition from a single-peaked distribution to the two-peaked structure can be clearly seen, and the essential features of the calculated results have been observed in the experimental intensity images (Fig. 2). Figure 4 shows cross sections of the single-peaked [Fig. 4(a)] and double-peaked [Fig. 4(b)] structures for both the measured NSOM images and the calculated distributions, each one normalized to its respective maximum intensity. Excellent qualitative agreement is observed. Quantitatively, the calculated single-peaked structure is narrower than the measured distribution, having a MFR of 2.73 μm when fitted by a Gaussian, compared with the measured MFR of 4.03 μm. This discrepancy is too large to be accounted for by the convolution of the physical size of the uncoated tip or by the increase in the upper cladding index that is due to the presence of the tip. Further research is needed. For the double-peaked structure, the peak-to-peak distance is calculated to be 7 μm, comparable to a measured value of 7.4 μm. The asymmetry in the NSOM image of the double-peaked structure can be explained by the presence of an antisymmetric mode propagating in the waveguide that arises if the pigtailing of the input fiber is off center. Figure 4(b) shows the calculated distribution for the case in which 5% of the power is launched into the lowest-order antisymmetric guided mode. The abrupt drop in intensity for the NSOM image 5 μm from the center of the distribution is due to the presence of the SiO_2 film that was used to define the waveguide in the APE process. The NSOM signal is negligible when the tip is over this film.

Multimode interference has been directly observed in a wide APE $LiNbO_3$ waveguide by use of a collection-mode NSOM. Light from a single-mode fiber launches power into multiple modes supported by the waveguide, which interfere along the length of the waveguide. The resulting periodic formation of double- and single-peaked intensity distributions is seen in the NSOM images. The agreement between the calculated intensity distribution and the NSOM results demonstrates that NSOM can be used for quantitative characterization of complex waveguide devices.

The authors thank M. H. Chou for the waveguide sample. A. L. Campillo acknowledges the support of the National Science Foundation (DMR-9802634). K. R. Parameswaran was supported by the Optoelectronic Materials Center Program, subcontract 3-17271-7810 (Prime Grant DARPA MDA972-00-1-0024), U.S. Air Force Office of Scientific Research grant F49620-99-1-0270, and the Stanford Optical Signal Processing Collaboration.

*Present address, Naval Research Laboratory, Washington, D.C., 20375; e-mail, alc@ccs.nrl.navy.mil.

References

1. L. B. Soldano and E. C. M. Pennings, J. Lightwave Technol. **13,** 615 (1995).
2. G. N. van den Hoven, A. Polman, G. van Dam, J. W. M. van Uffelen, and M. K. Smit, Opt. Lett. **21,** 576 (1996).
3. R. C. Reddick, R. J. Warmack, and T. L. Ferrell, Phys. Rev. B **39,** 767 (1989).
4. D. P. Tsai, H. E. Jackson, R. C. Reddick, S. H. Sharp, and R. J. Warmack, Appl. Phys. Lett. **56,** 1515 (1990).
5. G. H. Vander Rhodes, M. S. Ünlü, B. B. Goldberg, J. M. Pomeroy, and T. F. Krauss, Proc. IEEE Optoelectron. **145,** 379 (1998).
6. A. G. Choo, H. E. Jackson, U. Thiel, G. N. D. Brabander, and J. T. Boyd, Phys. Lett. **65,** 947 (1994).
7. G. H. Vander Rhodes, B. B. Goldberg, M. S. Ünlü, S. Chu, and B. E. Little, IEEE J. Sel. Top. Quantum Electron. **6,** 46 (2000).
8. A. L. Campillo, J. W. P. Hsu, C. A. White, and A. Rosenberg, J. Appl. Phys. **89,** 2801 (2001).
9. P. G. Suchoski, T. K. Findakly, and F. J. Leonberger, Opt. Lett. **13,** 1050 (1988).
10. M. H. Chou, I. Brener, M. M. Fejer, E. E. Chaban, and S. B. Christman, IEEE Photon. Technol. Lett. **11,** 653 (1999).
11. M. L. Bortz and M. M. Fejer, Opt. Lett. **16,** 1844 (1991).
12. P. Lambelet, A. Sayah, M. Pfeffer, C. Philipona, and F. Marquis-Weible, Appl. Opt. **37,** 7289 (1998).
13. R. Stockle, C. Fokas, V. Deckert, and R. Zenobi, Appl. Phys. Lett. **75,** 160 (1999).
14. J. W. P. Hsu, M. Lee, and B. S. Deaver, Rev. Sci. Instrum. **66,** 3177 (1995).
15. M. Lee, E. B. McDaniel, and J. W. P. Hsu, Rev. Sci. Instrum. **67,** 1468 (1996).
16. A. L. Campillo, "Near field scanning optical microscopy studies of photonic structures and materials," Ph.D. dissertation (University of Virginia, Charlottesville, Va., 2002).
17. M. S. Stern, IEEE Proc. Optoelectron. **135,** 56 (1988).